



ASSE-MEC-2014-XX

CFD Modeling of Flammable/Hazardous Gas Release and Dispersion for Risk and Safety Assessments

*Vladimir M. Agranat, PhD, President & Senior CFD Consultant
Applied Computational Fluid Dynamics Analysis (ACFDA)
Thornhill, Ontario, Canada*

*Sergei V. Zhubrin, PhD, VP R&D, Chief CFD Consultant
Applied Computational Fluid Dynamics Analysis
Thornhill, Ontario, Canada*

*Andrei V. Tchouvelev, PhD, CEO
A.V. Tchouvelev & Associates Inc.
Mississauga, Ontario, Canada*

*Zivorad Radonjic, Senior Environmental Meteorologist
ARCADIS SENES Canada Inc.
Richmond Hill, Ontario, Canada*

ABSTRACT

This paper is an attempt to give an overview of customized applications of general-purpose Computational Fluid Dynamics (CFD) software, PHOENICS, to the CFD modeling of flammable/hazardous gas release and dispersion (GRAD) performed by authors for risk and safety assessments. The three application areas are considered: safety of use of flammable gases (hydrogen, methane, etc.), single-phase pollutant dispersion and two-phase plume modeling for air quality assessments. The flammable GRAD CFD models developed and validated include the following features: the dynamic boundary conditions for sonic gas release from the tank/reservoir, the real gas law correlations at high operating pressures (Abel-Nobel equation of state), the local adaptive grid refinement for higher accuracy, customized turbulence models and special output capabilities. A single-phase CFD model for air quality assessments is briefly reviewed and compared with CALPUFF modeling results. A new two-phase homogeneous multi-group CFD model has been developed for prediction of drift drop plume behaviour. It was validated using the high quality data of 1977 Chalk Point Dye Tracer Experiment on water droplet deposition produced by a cooling tower. The model is recommended for analyses of two-phase plumes (polluted humid air,

dusted air, etc.) under low Stokes number conditions. The models developed are available as user-friendly templates for use by environmental and safety engineers.

KEYWORDS

Computational Fluid Dynamics (CFD)
PHOENICS Software
Flammable/Hazardous Gas
Gas Release and Dispersion (GRAD)
Two-phase Plume
Multi-group CFD Model
Risk and Safety Assessments

1. INTRODUCTION

Over the past 20 years, CFD modeling (see description of CFD approach in [1]) of flammable/hazardous GRAD has been used extensively in safety analyses and for air pollution assessments. CFD has been applied in risk and safety assessments in order to compliment the more traditional predictive methods such as AERMOD, CALPUFF and other models approved by the US Environmental Protection Agency (EPA) in the areas where these models demonstrate significant deficiencies (near-field dispersion, complex geometries, two-phase plumes,

wide buildings at non-perpendicular winds, etc.). The limitations of these models are described in [2, 3] and other recent papers.

In this paper, the three different CFD models and corresponding case studies are described:

- **advanced models of flammable GRAD** for safety analyses (use of hydrogen, methane, etc.);
- **a single-phase plume model** for air quality analyses;
- **a two-phase multi-group model** of drift drop plumes from cooling towers.

The above models have been developed, validated and applied to real-life industrial applications. They are based on customizing the commercial general-purpose CFD software, PHOENICS, by implementing the features/sub-models specific for each application area. PHOENICS is used as a framework and a solver. It has been validated and used around the world for more than 30 years. The documentation on PHOENICS is available in [4].

The user-friendly CFD templates have been prepared for each of the above three application areas to be used by environmental and safety engineers on regular basis. They contain the specific sub-models and supported by validation case studies.

2. CFD MODELING OF FLAMMABLE GRAD

CFD modeling of flammable GRAD with use of PHOENICS was described in detail in various papers including [5]-[14]. In these papers, the CFD was used to predict the extents of lower flammability level (LFL) clouds and the safe separation distances from sources/storages of flammable gas. The main focus was on the hydrogen safety applications, but the models developed are applicable to any flammable gas (methane, propane, etc.). Both subsonic and sonic releases in open, semi-enclosed and enclosed domains were considered in validation studies with steady-state and transient approaches. The major attention was paid to the model capability to accurately assess the safety distance from the release source based on the prediction of flammability envelope size and shape. The effects of orifice size, operating pressure, ambient conditions, ground surface and small barriers on the flammability envelope size were analyzed in simple and complex geometries. The user-friendly GRAD CFD model templates were prepared for applications by safety engineers in risk and safety assessments of processes involving the flammable gases.

The advanced flammable GRAD CFD models developed in [5]-[14] include the various specific features such as the dynamic boundary conditions for sonic gas release from the tank/reservoir, the real gas law correlations at high operating pressures (Abel-Nobel equation of state), the local adaptive grid refinement (LAGR) for higher accuracy, customized turbulence models and special output

capabilities. In this section, a few of advanced features of flammable GRAD CFD module are briefly described.

2.1 Dynamic Boundary Conditions

In general, the transient (dynamic) boundary conditions should be applied at the flammable gas release location in order to properly describe the released gas mass flow rate, which depends on time. Depending on the pressure in the gas storage tank, the regime of release could be subsonic or sonic (choked). Assuming the ideal gas law equation of state and a critical temperature at the leak orifice and solving the first-order ordinary differential equation for density, $\rho(t)$, the transient mass flow rate at the sonic regime of release could be approximated as [9,12]:

$$\dot{m}(t) = -V \frac{d\rho}{dt} = \rho(t)u(t)A \approx \dot{m}_0 e^{-\frac{C_d A}{V} t \sqrt{\gamma \left(\frac{2}{\gamma+1}\right)^{\frac{\gamma+1}{\gamma-1}} RT}},$$

$$\dot{m}_0 = C_d A \sqrt{\rho_0 P_0 \gamma \left(\frac{2}{\gamma+1}\right)^{\frac{\gamma+1}{\gamma-1}}} \quad (1)$$

where $u(t)$ is the flammable gas velocity at the leak orifice;

V is the tank volume; \dot{m}_0 , ρ_0 and P_0 are the flammable gas mass flow rate, the gas density in the tank and the gas pressure in the tank, respectively, at $t=0$; A is the leak orifice cross-sectional area; C_d is the discharge coefficient; and γ is the ratio of specific heats for flammable gas:

$\gamma = C_p / C_v$, with C_p and C_v being the specific heats at constant pressure and constant volume, respectively.

For example, for hydrogen ($\gamma=1.41$), the initial mass release rate calculated based on the second equation (1) is about 0.753 kg/s for a tank with a pressure of 400 bars, a 1/4" leak orifice and $C_d = 0.95$.

It should be noted that the choked release lasts until the ratio of the pressure in the tank over the ambient pressure, namely, P_0 / P_{am} is greater than or equal to $\left(\frac{\gamma+1}{2}\right)^{\frac{\gamma}{\gamma-1}}$ (it is about 1.90 for hydrogen).

2.2 Real Gas Law Properties

Under high pressure, flammable gases display gas properties different from the ideal gas law predictions. For example, at ambient temperature of 293.15°K and a pressure of 400 bars, the hydrogen density is about 25% lower than that predicted by the ideal gas law.

In order to account for real gas law behavior, the GRAD CFD module was provided with additional sub-models [9,12]. In particular, for hydrogen release and dispersion modeling the Abel-Nobel equation of state (AN-EOS) was used to calculate the hydrogen compressibility, z_{H_2} , in terms of empirical hydrogen co-density, d_{H_2} :

$$z_{H_2} = \frac{P}{\rho_{H_2} R_{H_2} T} = \left(1 - \frac{\rho_{H_2}}{d_{H_2}}\right)^{-1}, \quad (2)$$

where ρ_{H_2} , P , T and R_{H_2} are the compressed hydrogen density, pressure, temperature and gas constant, respectively. It should be noted that the hydrogen compressibility, z_{H_2} , is equal to 1 for the ideal gas law. The hydrogen gas constant, R_{H_2} , is 4124 J/(kgK). The hydrogen co-density, d_{H_2} , is about 0.0645 mol/cm³, or 129 kg/m³. Equation (2) can be simplified as:

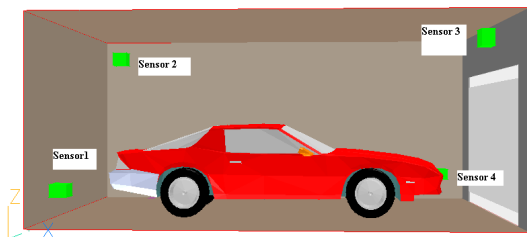
$$z_{H_2} = 1 + \frac{P}{d_{H_2} R_{H_2} T} \quad (3)$$

The AN-EOS accounts for the finite volume occupied by the gas molecules, but it neglects the effects of intermolecular attraction or cohesion forces. This equation accurately predicts the high-pressure hydrogen density behavior as shown in [9], where the AN-EOS was used for the CFD modeling of hydrogen release and dispersion from a 400-bar tank with the 1/4" orifice.

2.3 Local Adaptive Grid Refinement (LAGR)

A validation case simulated in [12] with use of LAGR is shown in Figure 1. The helium sub-sonic release in a garage with a car was considered in order to validate the flammable GRAD CFD model. The green blocks mark the locations of four helium sensors in the domain. The steady-state CFD predictions of helium concentrations at the sensor locations were compared with the experimental and numerical data published in [15].

Figure 1 - Geometry and Helium Sensors for Helium Subsonic Release in a Garage



LAGR was applied in this modeling case for higher accuracy of predictions. Table 1 taken from [12] shows that LAGR helps reduce significantly the predicted concentrations at the locations of Sensor 1 and Sensor 4, where the predictions made without LAGR are too high. The LAGR predictions are in a good agreement with the CFD simulations and experimental data reported in [15].

Table 1: Steady-state results for helium release in a garage with a car (k_gYEL turbulence model [4])

Simulations	Sensor 1	Sensor 2	Sensor 3	Sensor 4
Literature [15]	0.5%	2.55%	2.55%	1.0%
Initial coarse grid, 32×16×16	1.92%	2.53%	2.52%	1.94%
Adaptive refined, 39×26×24	0.98%	2.66%	2.62%	1.08%
Adaptive refined, 58×26×27	0.79%	2.70%	2.67%	1.01%

3. CFD MODELING OF SINGLE-PHASE PLUMES FOR AIR QUALITY ASSESSMENTS

Over the past two decades, CFD modeling of single-phase plumes has been widely used by many researchers for air quality analyses in addition to use of AERMOD, CALPUFF and other traditional analytical models as these models are insufficient and inaccurate in many cases (wide buildings, near-field regions, two-phase conditions, complex geometries, etc.). Some studies on comparing these models with CFD predictions are provided in [2, 3, 16] and other recent papers available in the literature. Also, a cross-validation work is possible with the combined use of CFD models and CALPUFF/AERMOD, etc.

In particular, the PHOENICS CFD software was applied in [16] in addition to CALPUFF in order to perform the near-filed modeling of pollutant dispersion around a backup diesel generating station in Dawson City, Yukon, Canada. This air quality assessment was completed in support of a permit renewal application for this generating station. Due to the fact that the plant is situated in a valley and experiences stagnant conditions each year that can inhibit the movement of air, the CALPUFF model was considered appropriate to determine the effect of plant emissions on community air quality. However, because it was also anticipated that building downwash would be a primary factor in determining maximum predicted contaminant concentrations in close proximity to the power house, a CFD modeling analysis was also undertaken to verify the accuracy of near-field CALPUFF modeling results. Based on the highest predicted concentrations from CALPUFF modeling, meteorological conditions conducive to building downwash were identified and selected for CFD modeling.

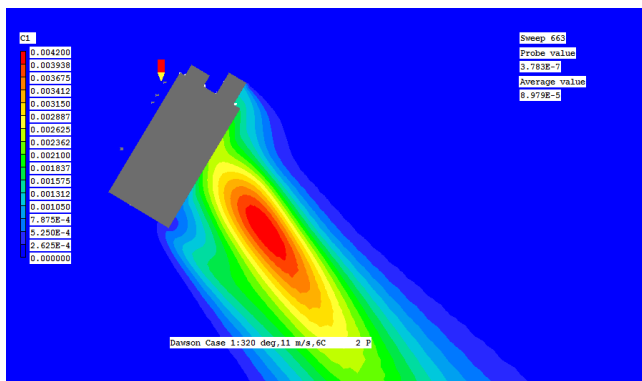
Figure 2 taken from [16] shows the geometry of the building housing the generation station and the stacks located on it. The diesel engines are housed in a low building (blue building on the left), vented through short, curved exhaust stacks such that the exhaust gas is released horizontally rather than vertically.

Figure 2 - Power Plant in Dawson City



Figure 3 shows a predicted contour of relative (with respect to a value at the source) mass fraction of contaminant, C1, in the worst case scenario. The area of maximum ground-level concentrations is shown in red.

Figure 3 - Ground-Level Contaminant Concentrations (Top View)



The CFD modeling results indicated that the predicted concentrations due to building downwash were closely correlated with wind speed, with the highest concentrations occurring with the highest wind speeds. The CFD

modeling results were consistent with those derived from the CALPUFF model, with CFD predicted maximum concentrations being less than 10% higher than those estimated using the CALPUFF model. However, whereas the CALPUFF model predicted the maximum point of impingement to occur at the facility property line beside the power house, the CFD model predicted the maximum concentrations to occur 10-20 meters from the property line.

The analysis provides justification for using the CALPUFF model to represent near-field contaminant concentrations in similar regulatory applications. Additional analysis would be required to verify whether the two models would continue to provide similar results for higher building heights, higher stacks or more complex building shapes.

4. CFD MODELING OF TWO-PHASE PLUMES WITH WATER DROPLET DEPOSITION

A new homogeneous two-phase multi-group CFD model was developed for analyses of two-phase plumes associated with the drift drop plumes from cooling towers. PHOENICS was customized by using its INFORM capability [4] to add user-defined sub-models. The model has been validated based on the high-quality Chalk Point Dye Tracer Experiment (CPDTE) described in [2, 17, 18]. A good agreement with experimental data on water deposition rates at selected locations from the cooling tower has been observed. It is better than that reported in [2, 17, 18]. The details of CFD model and case study are provided below in this section.

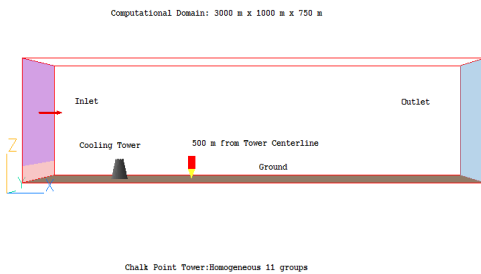
The conservation equations for mass fractions of water droplets having different sizes are solved in addition to the standard conservation equations for mixture mass, momentum, energy, water vapor mass fraction and turbulent quantities (turbulent kinetic energy and its dissipation rate). Extra terms are provided to the conservation equations for mass fractions of liquid water to account for the drift of water drops due to their gravitational settling. Various formulations for drift velocity and terminal velocity have been tested and compared. The phase change effects (condensation, evaporation, solidification and melting) are assumed to be negligible due to specific conditions of the experiment. The droplet-size distribution available at the cooling tower exit and containing the 25 groups of drops is simplified to 11 groups. Also, the 3-group and 1-group options are considered for comparison.

The individual drop deposition fluxes and the total deposition flux are calculated and compared with the experimental data available at the sensors located on the 35° arcs at 500 and 1000 m from the cooling tower centerline. The total deposition flux is calculated as a sum

of products of individual group mass concentrations of water drops and corresponding terminal velocities.

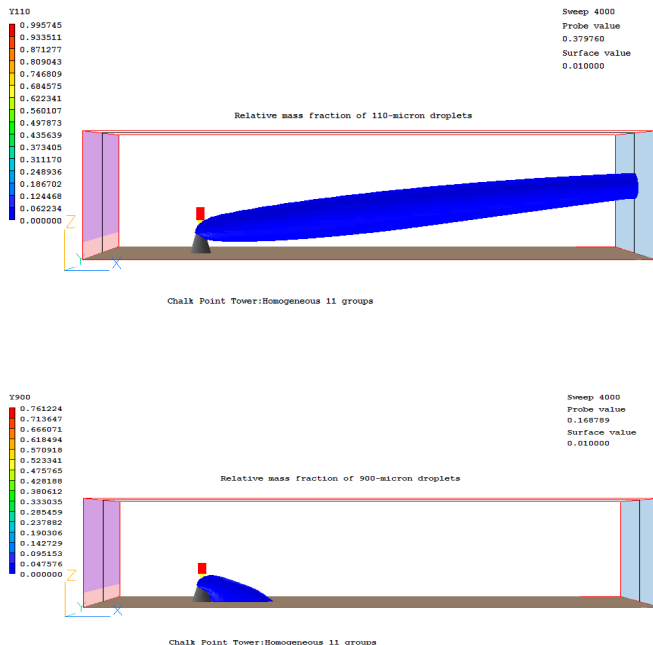
Figure 4 shows the computational domain, the cooling tower, the ground, the inlet and the outlet. The probe (a red pencil with yellow end) shows the location of the first measuring station (at a distance of 500 m from the cooling tower centerline).

Figure 4 - CFD Domain with Cooling Tower, Ground, Inlet and Outlet



The 1% iso-surfaces of relative mass fractions of 110- and 900-micron drops predicted with the 11-group distribution model are shown in Figure 5. It is seen that the 110-micron drops travel above the ground and leave the domain while the 900-micron drops fall on the ground at a certain distance from the cooling tower (smaller than 500 m).

Figure 5 - 1% Iso-surfaces of Relative Mass Fractions of 110-and 900-micron Drops (11-group Distribution)



The study has demonstrated a good agreement between the CFD predictions and the experimental data on the water vapor plume rise and the total drift deposition fluxes. In particular, the plume rise predictions agree well with experimental values (the errors are from 4% to 33% at different distances from the tower centerline). Table 2 shows the detailed comparison between the CFD predictions, the experimental data and the Briggs's formula available in [17].

Table 2: Predicted and measured plume rises at various distances from tower centerline

Distance from centerline (m)	Exp. plume rise (m)	Briggs's formula plume rise (m)	Plume rise predicted by CFD (778,050 cells, k-ε model) (m)
50	30	35 (17%)	40 (33%)
100	50	55 (10%)	48 (-4%)
200	100	87 (-13%)	72 (-28%)
500	N/A	160	121
1000	N/A	254	193

The CFD predicted maximum water deposition fluxes are in an agreement with the experimental values within a factor of 1.7, which is well within the industry acceptable error limits (a factor of 3) [2]. It is shown in Table 3 where the experimental data (last column) and the CFD results obtained on the two different grids are provided for comparison. The error factors are shown in bold.

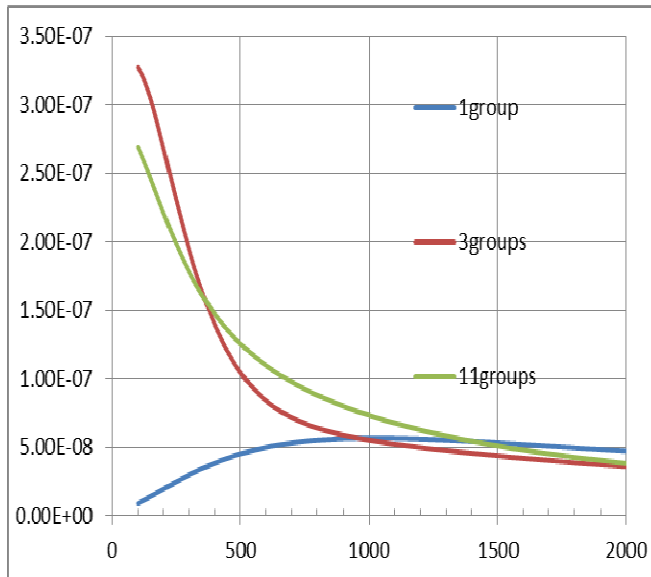
Table 3: Predicted and measured maximum water deposition fluxes at 500 and 1000 m from tower centerline (error factors are shown in bold)

Grid Size, (cell numbers)	Location, (m)	Predicted flux (3 groups) (kg/s/m ²)	Predicted flux (11 groups) (kg/s/m ²)	Exp. flux (kg/s/m ²)
212,500	500	1.22E-7 (0.90)	1.37E-7 (1.01)	1.36E-7
212,500	1000	5.72e-8 (1.27)	7.71e-8 (1.71)	4.52E-8
778,050	500	7.96e-8 (0.59)	1.12e-7 (0.82)	1.36E-7
778,050	1000	5.1e-8 (1.13)	6.81e-8 (1.51)	4.52E-8

It should be noted that the use of a few groups of drops is important for obtaining the accurate results. Figure 5 shows the comparison of water deposition fluxes predicted with use of 11-, 3- and 1-group options. It is seen that the 1-group results are not acceptable at short distances from the cooling tower (smaller than 500 m). They are very different from the 3- and 11-group results that are close to the

experimental data available at the distances of 500 and 1000 m (see Table 3).

Figure 5. Dependence of Water Deposition Flux (in $\text{kg/m}^2/\text{s}$) on Distance from the Tower (in m) Predicted with Different Options of Multi-group Model (11-group, 3-group and 1-group Options)



The CFD model developed is recommended for analyzing the drift drop plumes under the conditions similar to CPDTE conditions of small Stokes numbers. It is easier to use and not less accurate than the multiphase Eulerian-Lagrangian CFD model used recently in [2, 18] for modeling the CPDTE plume. The model developed has an advantage of being in a form fully compatible with methods widely used in CFD practice. The algebraic nature of the model relationships makes it easy bringing them into the computational loops of available predictive tools and, therefore, the model has a potential to supplant or complement the latter in the computational analysis of gravitational phenomena in engineering equipment and its environment.

5. CONCLUSIONS

The three CFD models have been developed, validated and applied to real-life industrial applications:

- **advanced models of flammable GRAD** for safety analyses (use of hydrogen, methane, etc.);
- **a single-phase plume model** for air quality analyses;
- **a two-phase multi-group model** for analyses of drift drop plumes from cooling towers.

The models are based on customizing the PHOENICS CFD software, which is used as a framework and a solver. The user-friendly CFD templates are available for applications

by environmental and safety engineers for risk and safety assessments.

REFERENCES

- [1] Versteeg, H.K. and Malalasekera, W. (1995). An Introduction to Computational Fluid Dynamics. Harlow, UK: Longman.
- [2] Meroney, R.N. (2006). CFD Prediction of Cooling Tower Drift. Journal of Wind Engineering and Industrial Aerodynamics, 94 (6), 463-490.
- [3] Schulman, L.L. and DesAutels, C.G. (2013). Comparing AERMOD and CFD Downwash Predictions for GEP Stacks. Proceedings of the Air & Waste Management Association's Conference Guideline on Air Quality Models: The Path Forward, Raleigh, North Carolina, USA, March 19-21, 2013, Control # 32.
- [4] PHOENICS On-line Information System: www.cham.co.uk/ChmSupport/polis.php.
- [5] Agranat, V., Cheng, Z. and Tchouvelev, A. (2004). CFD Modeling of Hydrogen Releases and Dispersion in Hydrogen Energy Station, Proceeding of the 15th World Hydrogen Energy Conference, Yokohama, Japan.
- [6] Tchouvelev, A., Howard, G. and Agranat, V. (2004). Comparison of Standards Requirements with CFD Simulations for Determining Sizes of Hazardous Locations in Hydrogen Energy Station, Proceeding of the 15th World Hydrogen Energy Conference, Yokohama, Japan.
- [7] Howard, G. W., Tchouvelev, A. V., Cheng, Z. and Agranat, V. M. (2005). Defining Hazardous Zones-Electrical Classification Distances, Proceeding of the 1st International Conference on Hydrogen Safety, Pisa, Italy.
- [8] Cheng, Z., Agranat, V. M. and Tchouvelev, A.V. (2005). Vertical Turbulent Buoyant Helium Jet - CFD Modeling and Validation, Proceeding of the 1st International Conference on Hydrogen Safety, Pisa, Italy.
- [9] Cheng, Z., Agranat, V. M., Tchouvelev, A. V., Houf, W. and Zhubrin, S.V. (2005). PRD Hydrogen Release and Dispersion, a Comparison of CFD Results Obtained from Using Ideal and Real Gas Law Properties, Proceeding of the 1st International Conference on Hydrogen Safety, Pisa, Italy.
- [10] Tchouvelev, A.V., Benard, P., Agranat, V. and Cheng, Z. (2005). Determination of Clearance Distances for Venting of Hydrogen Storage, Proceeding of the 1st International Conference on Hydrogen Safety, Pisa, Italy.
- [11] Cheng, Z., Agranat, V. M., Tchouvelev, A.V. and Zhubrin, S.V. (2005). Effectiveness of Small Barriers

as Means to Reduce Clearance Distances, Proceeding of the 2nd European Hydrogen Energy Conference, Zaragoza, Spain.

- [12] Agranat, V.M., Tchouvelev, A.V., Cheng, Z. and Zhubrin, S.V. (2007). CFD Modeling of Gas Release and Dispersion: Prediction of Flammable Gas Clouds. *Advanced Combustion and Aerothermal Technologies*, Edited by Syred, N. and Khalatov, A., Dordrecht, Netherlands: Springer, 179-195.
- [13] Tchouvelev, A.V, Cheng, Z., Agranat, V.M. and Zhubrin, S.V. (2007). Effectiveness of Small Barriers as Means to Reduce Clearance Distances. *International Journal of Hydrogen Energy*, 32 (10-11), 1409-1415.
- [14] Hourri, A., Angers, B., Bénard, P., Tchouvelev, A. and Agranat, V. (2011). Numerical Investigation of the Flammable Extent of Semi-confined Hydrogen and Methane Jets. *International Journal of Hydrogen Energy*, 36 (3), 2567-2572.
- [15] Swain, M. R., Schriber, J. A. and Swain, M. N., Addendum to Hydrogen Vehicle Safety Report: Residential Garage Safety Assessment. Part II: Risks in Indoor Vehicle Storage. Final Report.
- [16] Radonjic, Z., Agranat, V., Telenta, B., Hrebenyk, B., Chambers, D. and Ritchie, T. (2013). Comparison of Near-field CFD and CALPUFF Modelling Results around a Backup Diesel Generating Station. *Proceedings of the Air & Waste Management Association's Conference Guideline on Air Quality Models: The Path Forward*, Raleigh, North Carolina, USA, March 19-21, 2013, Control # 17.
- [17] Hanna, S.R. (1978), A Simple Drift Deposition Model Applied to the Chalk Point Dye Tracer Experiment. *Environmental Effects of Cooling Tower Plumes*, Symposium on, May 2-4, 1978, U. of Maryland, III-105-III-118.
- [18] Lucas, M., Martinez, P.J., Ruiz, J., Sanchez-Kaiser, A. and Viedma, A. (2010). On the Influence of Psychrometric Ambient Conditions on Cooling Tower Drift Deposition. *International Journal of Heat and Mass Transfer* 53 (4), 594-604.